Proceedings of the 28th IEEE
EMBS Annual International Conference
New York City, USA, Aug 30-Sept 3, 2006

Simulated Mossy Fiber Associated Feedforward Circuit Functioning as a Highpass Filter

Osbert C. Zalay, and Berj L. Bardakjian, *Member, IEEE*

***Abstract*—Learning and memory rely on the strict regulation of communication between neurons in the hippocampus. The mossy fiber (MF) pathway connects the dentate gyrus to the auto-associative CA3 network, and the information it carries is controlled by a feedforward circuit combining disynaptic inhibition with monosynaptic excitation. Analysis of the MF associated circuit using a mapped clock oscillator (MCO) model reveals the circuit to be a highpass filter.**

I. Introduction

THE hippocampus is a brain structure instrumental in learning and the formation of memories [1]–[3]. The CA3 region of the hippocampus has prolific recurrent excitatory connections between pyramidal neurons that are putatively responsible for auto-associative memory storage and recall [2], [4]. The ongoing processes of forming and retrieving memories require the CA3 to have flexibility and selectivity in its synaptic communications. Activity within the network is modulated by external inputs from the dentate gyrus (DG), via the mossy fiber (MF) pathway, and from the entorhinal cortex, via the perforant path (PP) [4], [5]. Research indicates that MF and PP inputs with the appropriate spatiotemporal encoding can effect both transient and long-term synaptic plasticity in the CA3 network [4]–[6]. In particular, granule cells (GC) from the DG have been shown to reliably detonate target cells in the CA3, essential for Hebbian learning and associative reinforcement (or depression) [3], [7]. Without input from the DG, learning in the CA3 is significantly impaired [8].

One important feature of the MF pathway is that it extends its excitatory afferents onto both excitatory and inhibitory cell types, namely glutamatergic pyramidal cells (PC) and γ-aminobutyric acid (GABA) releasing interneurons (IN), respectively [7], [9]–[11]. The ratio of GC-IN to GC-PC synapses is approximately 10:1 [9], suggesting a significant portion of the MF-CA3 network is devoted to inhibition. Not surprisingly, the majority of postsynaptic targets for GABAergic interneurons are pyramidal cells [11]. Given the large density of excitatory recurrent collaterals generating positive feedback amongst the pyramidal cell population in the CA3, the network is highly susceptible to hyperexcitability if unchecked [12], and is epileptogenic under pathological conditions [13]. Therefore, GC-PC synapses, known as mossy fiber terminals (which are characterized by giant boutons with multiple release sites), are balanced by a multitude of smaller, less potent GC-IN synapses, comprised of either *en passant* terminals or filopodial off-shoots of the giant MF boutons [5], [7], [9], [10], [12], [14]. A network architecture naturally emergent from this arrangement of synaptic connections is the feedforward inhibitory circuit [12], [15], [16]. For the MF-CA3 pathway, feedforward inhibition involves a disynaptic pairing of two components: the excitatory GC-IN synapse and the inhibitory IN-PC synapse. When this disynaptic circuit is combined with a GC-PC terminal, the net result is an MF associated feedforward circuit capable of mediating CA3 pyramidal cell activity in a manner dependent on GC action potential (AP) firing frequency [12], [16].

For this paper, we investigate the frequency dependent properties of the MF associated feedforward circuit using a nonlinear coupled-oscillator model to represent the network.

II. Modeling the Feedforward Circuit

The model proposed in this paper is a variant of the Mapped Clock Oscillator (MCO) model first proposed by Bardakjian [17] to simulate cellular electrical rhythms. The MCO is a hybrid system encompassing a dynamic core of nonlinear differential equations in phase, ϕ, and amplitude, α, mapped to a static nonlinearity, $y(\alpha,\phi)$, that generates an observable output (e.g. voltage). The static nonlinearity captures the salient features of cellular electrical waveforms, thereby reducing the complexity of the preceding dynamic stage. This approach is an extension of the Wiener linear-nonlinear cascade [18] to a dual nonlinear cascade.

The MCO model also incorporates input portals that accommodate internal network coupling as well as external stimuli [17], [19]. There are four categories of portals, each portraying a separate, lumped mechanism for coupling or stimulation: the α-portal modulates the amplitude, simulating the effect of ion/ligand concentrations on cellular membrane processes; the ϕ-portal affects the rate of change of phase (which translates to neuronal firing rate), representing electric-field coupling or stimulation; the ρ-portal handles synaptic coupling, which changes the resting level and governs amplitude-to-firing-frequency encoding;

Manuscript received April 3, 2006. This work was supported in part by grants from the Canadian Institutes of Health Research and the Natural Sciences and Engineering Research Council of Canada.

B. L. Bardakjian is the corresponding author, and is cross-appointed to the Department of Electrical and Computer Engineering and the Institute for Biomaterials and Biomedical Engineering at the University of Toronto, Toronto, ON, M5S 3G9, Canada (phone: 416-978-6552; fax: 416-978-4317; e-mail: berj@ cbl.utoronto.ca).

and the γ-portal portrays electrotonic coupling. To replicate the essential layout of the MF associated feedforward circuit, 3 labile MCOs – each representing a different class of neuron belonging to the circuit – were coupled synaptically as illustrated in Fig. 1. The labile MCO has the property of producing an observable output only when stimulated above threshold, whereas the conventional MCO generates a rhythmic output that is sustained in the absence of any input [19].

A. Oscillator Dynamics

The dynamic equations of the labile MCO are presented here in polar form:

$$\dot{\alpha} = k_\alpha \alpha^m (v(x) - \alpha^n) + S_{\gamma 1} \sin(\phi) + S_{\gamma 2} \cos(\phi) \qquad (1)$$

$$\dot{\phi} = \omega(1 + R(\phi) \cdot S_\phi) + \frac{1}{\alpha}\left(S_{\gamma 1} \cos(\phi) - S_{\gamma 2} \sin(\phi)\right) \qquad (2)$$

where m = 1/3, n = 2, and $k_\alpha = 10^3$ s^{-1}. Both α and ϕ are dimensionless quantities, and ϕ is bounded between 0 and 2π. The intrinsic angular frequency, ω (rad/s), is a constant that determines the unperturbed firing rate of the model neuron. S_β is the input to the β-portal, where $\beta = \{\alpha, \phi, \rho, \gamma_1, \gamma_2\}$, and is normalized to be dimensionless. $S_{\gamma 1} = S_{\gamma 2} = 0$ because we do not consider electrotonic coupling in the MF associated feedforward circuit. $R(\phi)$ is a refractory function of the highpass Butterworth type, with unity gain and a filter order of 4. Its cutoff is set to $\phi_c = 4\pi/5$, so that the oscillator remains insensitive to ϕ-portal inputs for the refractory portion of the cycle ($\phi < \phi_c$). The threshold function, $v(x)$, is a sigmoid whose expression

$$v(x) = \frac{1}{1 + \exp\{-v_1(x - v_2)\}} \qquad (3)$$

has parameters v_1 = 30 and v_2 = 0.5. Its dimensionless argument, x, combines inputs from the α- and ρ-portals:

$$x = K_\alpha S_\alpha + K_\rho A(S_\rho) \qquad (4)$$

with K_α and K_ρ (V^{-1}) as constants that weight the relative contributions of each input. The alpha-function, $A(S_\rho)$, is a function that transforms and integrates the ρ-portal input in a fashion that mimics the electrophysiological action of the synapse. The alpha-function is written explicitly as

$$A(S_\rho(t)) = \sigma' \int_{t_0}^{t} S_\rho(u) \cdot a(t-u) \exp\{1 - a(t-u)\} du \qquad (5)$$

and it has units of voltage. The time interval of integration is $t - t_0$ seconds. σ' (V·s^{-1}) is a scaling factor, and a (s^{-1}) is a constant controlling the time-dependent properties of the integrand.

The dynamic MCO elements are solved simultaneously using Gear's method [20], a variable-step algorithm capable of integrating systems of stiff, nonlinear ODEs.

B. The Static Nonlinearity

The static nonlinearity maps the phase and amplitude to a measurable quantity, which in this case is the transmembrane voltage of the model neuron:

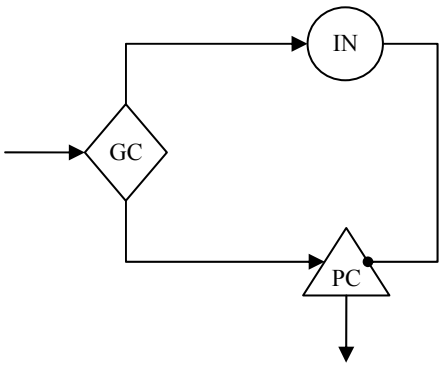

Fig. 1. Schematic of the mossy fiber (MF) associated feedforward circuit. The granule cell (GC) receives a DC input that stimulates it to generate a train of action potentials at a select frequency. The excitatory GC output is directed to two postsynaptic targets: a pyramidal cell (PC) and an interneuron (IN). The interneuron completes the circuit with an inhibitory synapse onto the PC.

$$y(\alpha, \phi) = a_0 + A(S_\rho) + \alpha \cdot W(\phi). \qquad (6)$$

a_0 is the DC offset (approximate neuronal resting level), and $W(\phi)$ is the *intrinsic waveform*. $W(\phi)$ has no analytical expression; it is sampled from the time-dependent voltage profile of a cell-type's distinctive action potential waveform, normalized as a function of phase only. Because the electrical waveform generated by a particular cell-type differs from that of another, the waveform is deemed to be *intrinsic*. The values of $W(\phi)$ are derived from whole-cell patch-clamp recordings and stored in a look-up table referenced by phase values ranging from 0 to 2π.

C. Input Portals and Coupling

The α-, ϕ- and ρ-portals take, as inputs, the outputs of MCOs via their static nonlinearities, as well as external stimuli. The algebraic expressions for these three portals feeding the n-th MCO in a network of M MCOs are as follows: letting $m = \{1, 2, \ldots, M\}$ and $\hat{y} = y(\alpha, \phi) - a_0$,

$$S_{\alpha,n}(t) = \sum_m^M \left(\frac{c_{\alpha,mn} \cdot \hat{y}_m}{\sigma_n} \right) + S_{\alpha,n}^{ex}(t), \qquad (7)$$

$$S_{\phi,n}(t) = \sum_m^M \left(\frac{c_{\phi,mn} \cdot \hat{y}_m}{\sigma_n} \right) + \varepsilon_n \frac{A_n(S_{\rho,n}(t))}{\sigma_n''} + S_{\phi,n}^{ex}(t) \qquad (8)$$

and

$$S_{\rho,n}(t) = \sum_m^M \left(\frac{c_{\rho,mn} \cdot v(\hat{y}_m) \cdot \hat{y}_m}{\sigma_n} \right) + S_{\rho,n}^{ex}(t). \qquad (9)$$

$c_{\beta,mn}$ is the coupling factor denoting the strength of the connection from the m-th MCO to the β-portal of the n-th MCO, $\beta = \{\alpha, \phi, \rho\}$. The coupling factors have a range of 0 (no coupling) to ±1 (full coupling), where the sign depends on whether the connection is excitatory or inhibitory. For the MF associated feedforward circuit, coupling values are listed in Table 1. S_β^{ex} is the external input to the β-portal. σ is

a normalization factor and is the root-mean-square value of $W(\phi)$ from (6); $\sigma'' = \sigma/10$. Amplitude-to-frequency encoding is made possible by the alpha-function term in (8), which is multiplied by an encoding constant, ε, that defines the firing frequency sensitivity of a neuron to synaptic inputs, and can assume values from 0 to 1. Finally, $v(\hat{y})$ from (9) is a sigmoid of the form given by (3), and acts as a threshold function for screening out ρ-portal inputs that are not considered action potentials, so that $A(S_\rho)$ only sums spikes.

TABLE I
MF FEEDFORWARD CIRCUIT COUPLING FACTORS

			n		
			1	*2*	*3*
c_α	*m*	*1*	0	0.01	0.01
		2	0.01	0	0.01
		3	0.01	0.01	0
c_ϕ	*m*	*1*	0	0.01	0.01
		2	0.01	0	0.1
		3	0.01	0.1	0
c_ρ	*m*	*1*	0	0	0
		2	0.45	0	-0.40
		3	0.5	0	0

m and *n* are source and destination neurons, respectively. MF associated neurons are numbered accordingly: 1 – granule cell; 2 – pyramidal cell; 3 – interneuron.

III. RESULTS

The properties of the MCO simulated MF associated feedforward circuit were investigated by stimulating the GC through its ρ-portal and observing the output of the circuit from the pyramidal cell.

A. Feedforward Inhibition

To ascertain the functional characteristics of disynaptic feedforward inhibition in the MF associated network, a pair of simulation runs was performed: one with the inhibitory interneuron deleted from the circuit, and the other with the interneuron connected in its proper place. In both instances, the granule cell was prompted to fire action potentials at a moderately low rate of 8 Hz. (Most GCs have firing frequencies below 1 Hz until strongly stimulated [16].) Fig. 2 displays the results of the simulations. For the case in which the interneuron was removed, GC action potentials induced APs in the pyramidal cell, demonstrating unencumbered suprathreshold excitation. The PC postsynaptic potentials (PSPs), as generated by the alpha-function in (5), were monophasic and excitatory. Conversely, GC firing did not invoke a single pyramidal AP when the interneuron was connected in the circuit, and the PSPs that were produced were biphasic with a pronounced hyperpolarization phase.

B. Frequency Response of the Feedforward Circuit

The frequency-dependence of the MF associated feedforward circuit was examined by varying the firing frequency of the granule cell between 0 and 50 Hz. This

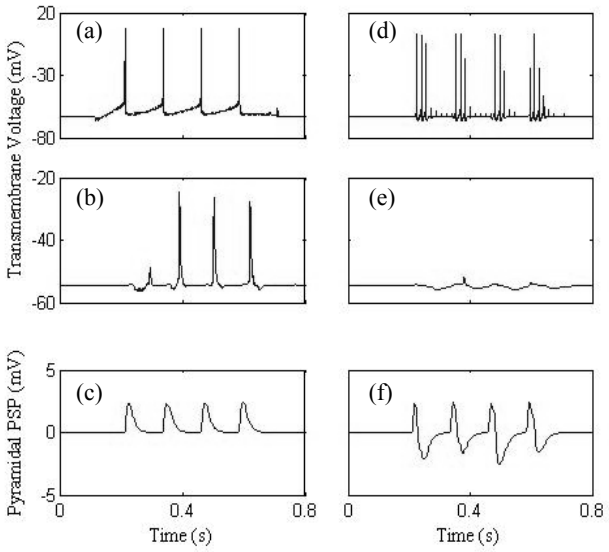

Fig. 2. Role of the interneuron in the MF associated feedforward circuit. (a) Granule cell action potentials. (b) Pyramidal cell response to the excitatory drive from the granule cell in the absence of inhibition. (c) Non-biased pyramidal excitatory PSP train from the GC-PC synapse. (d) Limited bursting of the interneuron in response to granule cell excitation. (e) Pyramidal cell output resulting from GC firing with the inhibitory interneuron included in the feedforward circuit. Action potentials were completely suppressed. (f) Biphasic PSPs (non-biased) are recorded in the pyramidal cell combining the effects of both GC-PC (excitatory) and IN-PC (inhibitory) synapses.

frequency range is within the physiological spectrum of the GC [7]. The variation was achieved by changing the oscillator's intrinsic angular frequency, ω (refer to (2)), a more direct and controlled method than changing the level of DC stimulation to the ρ-portal, then relying on amplitude-to-frequency encoding at the ϕ-portal, as dictated by (8).

Increasing GC firing frequency led to a marked transition in circuit behavior, from overall suppression of the pyramidal cell at low frequencies to facilitation of its activity at frequencies exceeding 10 to 15 Hz. Beyond 20 Hz, PC action potentials were regularly elicited, in spite of feedforward inhibition.

For a circuit response that was inhibitory, the pyramidal cell's postsynaptic potential (with DC bias subtracted) was mostly negative. The opposite was true for an excitatory response. To quantify the level of excitation or inhibition at the output, the pyramidal PSP was integrated numerically (using the trapezoidal method) for each value of GC frequency tested. The resultant plot, depicted in Fig. 3, reveals the frequency response of the MF associated feedforward circuit approximates that of a highpass filter.

IV. DISCUSSION

There are many examples in Nature of systems in which opposing forces are at play, and tipping the system in favor of one particular force allows that force to determine the system's fate. The MF associated feedforward circuit is one such example, where inhibition and excitation compete for dominance, and depending on the circumstances, either

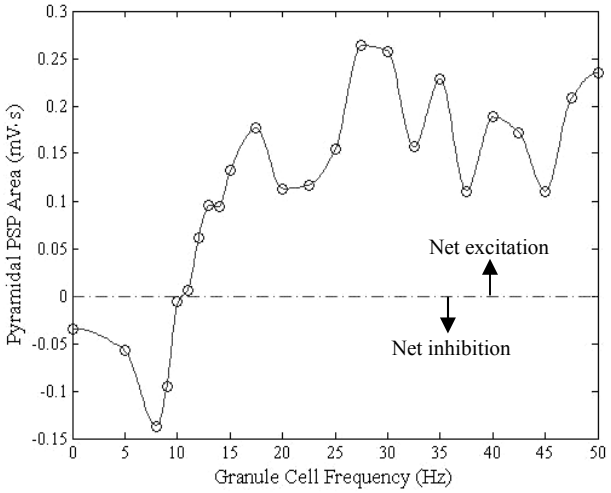

Fig. 3. Frequency-dependent switching of the MF-associated feedforward circuit from inhibition to excitation. Pyramidal cell PSPs were integrated with respect to time to get the total PSP area in response to the granule cell firing tonically for 500 ms, except for the first run in which the PSP area was calculated for a single evoked GC action potential (0 Hz). A negative PSP area represents a net inhibitory response, while a positive area represents net excitation. The circuit switches from net inhibition to net excitation as granule cell firing frequency increases past 10 Hz.

inhibition or excitation prevails, dictating circuit behavior.

The results of the MCO model demonstrate the MF associated feedforward network acts as a highpass filter for inputs originating from the dentate gyrus. As Fig. 3 indicates, the filter is non-ideal, exhibiting Gibbs phenomenon and ripples in the pass-band. The degree of non-ideality in biological MF feedforward circuits has not been characterized and cannot be gauged from the model.

Another limitation of our setup is that it consists of 3 model neurons, whereas the true network constituents are far more numerous, arrayed in sub-populations of functionally-similar neurons [11], [12]. However, the fundamental connectivity of the feedforward circuit remains as is shown in Fig. 1, and the 3 labile MCOs can be considered high-level representations of those neuronal sub-populations. This simplification does not detract from the model's ability to make predictions about network properties. In comparison with electrophysiological investigations of the MF feedforward circuit, the MCO model was able to verify many of the experimental observations, including the biphasic nature of the pyramidal PSPs (Fig. 2) [12], [16] and the frequency- dependent switching from inhibition to excitation for GC frequencies greater than 10 Hz [7], [12].

Altogether, evidence from the model and from experiment suggests the MF associated feedforward circuit plays an important regulatory role in auto-associative learning and information processing in the hippocampus, reserving access to the sensitive recurrent collaterals of the CA3 for those DG inputs that carry the appropriate temporal code.

ACKNOWLEDGMENT

The authors of this paper thank the past and present members of the Carlen lab, at the Toronto Western Research Institute, who provided us with data from patch-clamp recordings of rat hippocampal neurons for use in our model.

REFERENCES

[1] H. Eichenbaum, "A cortical-hippocampal system for declarative memory," *Nature Rev. Neurosci.*, vol. 1, no. 1, pp. 41–50, Oct. 2000.

[2] M. E. Hasselmo, E. Schnell, and E. Barkai, "Dynamics of learning and recall at excitatory recurrent synapses and cholinergic modulation in rat hippocampal region CA3," *J. Neurosci.*, vol. 15, no.7, pp. 5249–5262, July 1995.

[3] B. L. McNaughton and R. G. M. Morris, "Hippocampal synaptic enhancement and information storage within a distributed memory system," *Trends in Neurosci*., vol. 10, no. 10, pp. 408–415, Oct. 1987.

[4] D. B. T. McMahon and G. Barrionuevo, "Short- and long-term plasticity of the perforant path synapse in the hippocampal area CA3," *J. Neurophysiol.*, vol. 88, pp. 528–533, July 2002.

[5] D. A. Henze, N. N. Urban, and G. Barrionuevo, "The multifarious hippocampal mossy fiber pathway: a review," *Neuroscience*, vol. 98, no. 3, pp. 408–427, June 2000.

[6] K. Kobayashi and M. Poo, "Spike train timing-dependent associative modification of hippocampal CA3 recurrent synapses by mossy fibers," *Neuron*, vol. 41, pp. 445–454, Feb. 2004.

[7] D. A. Henze, L. Wittner, and G. Buzsáki, "Single granule cells reliably discharge targets in the hippocampal CA3 network *in vivo*," *Nature Neurosci.*, vol. 5, no. 8, pp. 790–795, Aug. 2002.

[8] B. L. McNaughton, C. A. Barnes, J. Meltzer, and R. J. Sutherland, "Hippocampal granule cells are necessary for normal spatial learning but not for spatially-selective pyramidal cell discharge," *Exp. Brain Res.*, vol. 76, no. 3, pp. 485–496, Aug. 1989.

[9] L. Acsády, A. Kamondi, A. Sik, T. Freund, and G. Buzsáki, "GABAergic cells are the major postsynaptic targets of mossy fibers in the rat hippocampus," *J. Neurosci.*, vol. 18, no. 9, pp. 3386–3403, May 1998.

[10] J. Bischofberger and P. Jonas, "TwoB or not twoB: differential transmission at glutamatergic mossy fiber–interneuron synapses in the hippocampus," *Trends in Neurosci.*, vol. 25, no. 12, pp. 600–603, Dec. 2002.

[11] I. Vida and M. Frotscher, "A hippocampal interneuron associated with the mossy fiber system," *Proc. Nat. Acad. Sci.*, vol. 97, no. 3, pp. 1275-1280, Feb. 2000.

[12] J. J. Lawrence and C. J. McBain, "Interneuron diversity series: containing the detonation – feedforward inhibition in the CA3 hippocampus," *Trends in Neurosci.*, vol. 26, no. 11, pp. 631–639, Nov. 2003.

[13] P. A. Schwartzkroin and D. A. Prince, "Cellular and field potential properties of epileptogenic hippocampal slices," *Brain Res.*, vol. 147, no. 1, pp. 117–130, May 1978.

[14] J. J. Lawrence, Z. M. Grinspan, and C. J. McBain, "Quantal transmission at mossy fiber targets in the CA3 region of the rat hippocampus," *J. Physiol.*, vol. 554, no. 1, pp. 175–193, Jan. 2004.

[15] M. Frotscher, "Mossy fiber synapses on glutamate decarboxylase-immunoreactive neurons: evidence for feed-forward inhibition in the CA3 region of the hippocampus," *Exp. Brain Res.*, vol. 75, no. 2, pp. 441–445, Apr. 1989.

[16] M. Mori, M. H. Abegg, B. H. Gähwiler, and U. Gerber, "A frequency-dependent switch from inhibition to excitation in a hippocampal unitary circuit," *Nature*, vol. 431, pp. 453–456, Sept. 2004.

[17] B. L. Bardakjian and N. E. Diamant, "A mapped clock oscillator model for transmembrane electrical rhythmic activity in excitable cells," *J. Theor. Biol.*, vol. 166, pp. 225–235, Feb. 1994.

[18] I. W. Hunter and M. J. Korenberg, "The identification of nonlinear biological systems: Wiener and Hammerstein cascade models," *Biol. Cybernetics*, vol. 55, no. 2–3, pp. 135–144, Nov. 1986.

[19] J. Zariffa and B. L. Bardakjian, "Neuronal electrical rhythms described by composite mapped clock oscillators," *Ann. Biomed. Eng.*, vol. 34, no. 1, pp. 128–141, Jan. 2006.

[20] C. W. Gear. The automatic integration of ordinary differential equations. Comm. ACM, vol. 14, no. 3, pp. 176–179, Mar. 1971.